Effect of displacement rate and curing conditions on the fracture behaviour of crosslinked epoxy systems

V.-T. Truong
Materials Research Laboratory, DSTO Melbourne, PO Box 50, Ascot Vale, Victoria 3032, Australia
(Received 11 June 1989; revised 15 November 1989; accepted 22 November 1989)

The fracture behaviour of unmodified and rubber-modified epoxies from the diglycidyl ether of bisphenol A epoxy cured with piperidine has been investigated as a function of displacement rate (or crack propagation velocity). Failure modes type B (unstable stick/slip) and type C (brittle stable) were observed in the unmodified epoxies, but the fracture behaviour shifted to type A (ductile stable) as the rubber content increased. In the rubber-modified epoxies, the rubber second phase did not have a large influence on the fracture toughness but tended to stabilize the crack propagation, i.e. increase the displacement rate at which the mode changes from type A to type B. A high cure temperature substantially improved the fracture behaviour of the rubber-modified epoxies, giving a very high stress intensity factor (4 MN $m^{-3/2}$) and further stabilizing the crack propagation. For resins of the same cure cycle, but different rubber content, the crack opening displacement and Dugdale plastic zone size were found to be constant at the type A/type B transition. Type B fracture is an alternation of type A and type C fracture.

(Keywords: epoxy resins; crack opening displacement; crack propagation velocity; fracture mode transition; plastic zone)

INTRODUCTION

Epoxies have been widely used as structural adhesives and matrix materials for composites in the aerospace industry, and as potting and encapsulating materials for the electronics industry. The use of epoxies has recently been extended to the automotive and building industries. The extensive application of epoxies in some critical areas that require toughness and structural durability has aroused considerable interest in their mechanical properties. In particular, in the past decade a large number of studies have aimed to modify these brittle crosslinked materials and investigate the fracture mechanisms of unmodified and rubber-modified epoxies. Indeed, from a structural design and engineering viewpoint, an understanding of crack propagation and toughening mechanisms is absolutely essential.

It has been demonstrated that, as the test temperature decreases or the strain rate increases, the mode of fracture can change from ductile propagation (type A) to stick/slip propagation (type B) and then to brittle propagation (type C)[1,2]. This behaviour can be quantitatively explained by the crack-tip blunting model proposed by Kinloch and Williams[3], who considered the effect of temperature and strain rate on material yield behaviour at the crack tip. The model predicts that enhancement of the stress intensity factor at initiation (K_{Ici}) of the stick/slip propagation is due to blunting at the crack tip, which is facilitated by the low yield stress. In fact, it has been experimentally demonstrated that the stress intensity factor K_{Ic} decreases rapidly as the yield stress increases in several epoxy systems[2,4]. Moreover, the crack opening displacement δ_c rises rapidly when the fracture mode changes from type C to type B[5]. These observations have confirmed that plasticity of the material at the crack tip is the controlling factor of the blunting mechanism and therefore of the fracture toughness of epoxies.

The similar effects of testing rate and temperature on the fracture behaviour imply viscoelastic characteristics in crack propagation. The equivalence between rate and temperature has been quantitatively described by Hunston *et al.*[6]. They have determined values of the shift factor a_T for the time–temperature superposition and found that a_T is independent of the epoxy composition. Using the shift factor a_T and the time to failure t_f, Kinloch and Hunston[7] have successfully established master curves of fracture energy against the reduced time t_f/a_T for a number of epoxy systems. Although a considerable amount of data have demonstrated the existence of time–temperature correlation in epoxy fracture processes, most of the data have been concentrated on the fracture behaviour in type B and type C regimes, and type A has not been investigated in detail. In fact, the effects of rate and temperature have been simultaneously examined by Kinloch *et al.*[2], but only three displacement rates ranging from 10^{-7} to 10^{-4} m s^{-1} were employed and few type A fracture data were observed due to the limits of the test temperature.

The addition of liquid rubber to an epoxy resin has been considered as the most convenient and effective method to enhance its fracture toughness, but other modifications are possible. Different cure temperatures and gel temperatures can induce a variety of second-phase morphologies from the same epoxy formulation and thus different mechanical properties and stress response mechanisms[8,9]. The cure cycle, therefore, is another important factor in obtaining optimum properties for epoxies. Further, the molecular weight between

0032-3861/90/091669-09

crosslinks (M_c) can be controlled by using different amine/epoxy reactant ratios or difunctional epoxy prepolymers with different molecular weights. LeMay *et al.*[10] found that the fracture energies of unmodified epoxies are closely proportional to $M_c^{1/2}$. Pearson and Yee[11] studied the M_c-dependent fracture toughness of unmodified and rubber-modified epoxies and observed that increasing M_c leads to a small increase in the energy release rate G_{Ic} of the unmodified specimens, similar to the results obtained by LeMay *et al.*[10], but to a substantial increase in G_{Ic} of the rubber-modified epoxies. Recently, Kinloch *et al.*[12] have reported an enhancement in toughness by increasing the cure temperature and shortening the period of cure. They related the higher toughness to a larger M_c, indirectly determined via the equilibrium rubbery modulus E_r.

The purpose of this study is to investigate the effect of the cure temperature and the displacement rate on the fracture toughness and the transition between the fracture modes of unmodified and rubber-modified epoxies from the diglycidyl ether of bisphenol A with piperidine. Modes of fracture and dependence of the plastic zone size and the crack opening displacement on the rubber content and the cure temperature will be discussed.

EXPERIMENTAL

Materials

The epoxy resin was a diglycidyl ether of bisphenol A (DGEBA, Epikote 828 from Epirez Australia Pty Ltd) cured with piperidine. The liquid rubber (Hycar 1300 X8 from B. F. Goodrich Pty Ltd) was a carboxyl-terminated random copolymer of butadiene and acrylonitrile (CTBN), containing 17% acrylonitrile, of molecular weight 3500. The preparation of the unmodified and rubber-modified epoxies has been described in a previous report[1]. Formulations of the test specimens are shown in *Table 1*. Two cure cycles were conducted: (1) 120°C/16 h and (2) 150°C/2.5 h then 120°C/16 h. In each the post-cure was 150°C/2 h.

Crosslink density

The extrapolated onset and end of the glass transitions of the samples were measured at a heating rate of 10°C min^{-1} by differential scanning calorimetry using a DuPont model 1090 Thermal Analyzer. The samples (about 1 mm thick, 10 mg) were cut from the casting to give a moulded flat surface, and were cooled rapidly from just about the transition to erase annealing and ageing effects before the measuring run. The glass transition temperature T_g was taken as the mean of the range.

The equilibrium rubbery modulus E_r was measured at 140 and 160°C by a dynamic mechanical thermal analysis unit (DMTA, Polymer Laboratories Ltd) at a frequency of 1 Hz and a heating rate of 2°C min^{-1}. The analysis was conducted over the temperature range 30 to 160°C. The specimen dimensions were $30 \times 10 \times 1.2$ mm^3.

Table 1 Formulation of test specimens

	Unmodified epoxy	Rubber-modified epoxy
Epoxy resin (phr)[a]	100	100
Piperidine (phr)	5	5
CTBN (phr)	0	5 or 10 or 15

[a] phr = parts per hundred resin by weight

The value of M_c can be derived from T_g (K) by[13]:

$$T_g = T_{g0} + C/M_c \quad (1)$$

or from E_r (N m^{-2})[13] by:

$$\log_{10}(E_r/3) = 6 + 293d/M_c \quad (2)$$

where T_{g0} is the T_g of uncrosslinked epoxy (259 K)[14], C is a constant (3.9×10^4)[13] and d is the density of the epoxy (1.18 g cm^{-3}).

Fracture toughness and crack propagation velocity

The stress intensity factor K_{Ic} was determined by double torsion (DT) geometry[15]. The DT specimens, which were machined from sheets of the materials, have the dimensions $30 \times 75 \times 4$ mm^3. A groove 1.5 mm deep was machined onto one surface of the specimen along the central line. At one end of the groove a notch was made with a handsaw and a short sharp crack was created by a razor blade. The specimen was mounted on a DT jig attached to a universal testing machine (Instron model 1121). The K_{Ic} values were measured at displacement rates $\dot{y}$ ranging from 8.3×10^{-7} to 8.3×10^{-3} m s^{-1} at room temperature (22±2°C). K_{Ic} was determined by[16]:

$$K_{Ic} = \frac{Pl}{[kwt^3 t_n(1-\nu)]^{1/2}} \quad (3)$$

where P is the load, l is the arm moment length (10.75 mm), w is the specimen width, t is the specimen thickness, t_n is the crack plane thickness (i.e. the specimen thickness less the groove depth), k is a constant depending[16] on the ratio of w/t, and ν is Poisson's ratio (=0.35).

In addition, four DT specimens of $46 \times 90 \times 7.5$ mm^3 and $76 \times 150 \times 11$ mm^3 were made to ensure that the 4 mm samples were thick enough to satisfy plane-strain conditions. According to ASTM E399-83, the required thickness is at least $2.5(K_{Ic}/\sigma_{ty})^2$, where σ_{ty} is the tensile yield stress. Thus, the required thickness is approximately 11 mm for $K_{Ic} = 4$ MN $m^{-3/2}$ and $\sigma_{ty} = 60$ MN m^{-2}. The K_{Ic} values for specimens containing 15 phr of rubber cured by cycle (2), at $\dot{y} = 1.67 \times 10^{-5}$ m s^{-1}, were 3.80±0.08, 4.15±0.20 and 3.75±0.05 MN $m^{-3/2}$ for the thickness of 4, 7.5 and 11 mm, respectively. Accordingly, the fracture toughness is largely insensitive to specimen thickness and the fracture data obtained with specimens 4 mm thick satisfy the plane-strain conditions. It has been reported that fracture data from DT specimens one-quarter to one-half of the minimum recommended thickness yield valid data comparable with results obtained from compact tension specimens and double cantilever beams[17,18].

The crack propagation velocity $\dot{a}$ of type A fracture growth was calculated by using the crack length Δa during the time of propagation Δt, i.e. $\dot{a} = \Delta a/\Delta t$, and was varied by changing $\dot{y}$.

Yield stress

Cylindrical samples (12.5 mm diameter × 25 mm) were tested in compression to give the true stress σ_{cy} as a function of strain rate $\dot{e}$. The strain rate $\dot{e}$ was obtained from the displacement rate $\dot{y}$. The true compressive yield stress σ_{cy} was estimated by:

$$\sigma_{cy} = (P_y/A_0)(1-e_y) \quad (4)$$

where P_y is the load at yield, A_0 is the initial

cross-sectional area, and e_y is the yield strain. The true compressive yield stress σ_{cy} was converted to the true tensile yield stress σ_{ty} by using the ratio of the tensile to the compressive yield stress ($\sigma_{ty}/\sigma_{cy}=3/4$)[19].

Young's modulus

Young's modulus E was determined at five different strain rates (2.6×10^{-6}, 10^{-5}, 10^{-4}, 10^{-3} and 10^{-2} s^{-1}) with a rectangular bar of $80\times15\times4$ mm^3 using a three-point bend test. The value of E is given by:

$$E=L^3P/(4ybt^3) \quad (5)$$

where L is the distance between the supports, P is the load, y is the displacement, b is the breadth and t is the thickness.

RESULTS AND DISCUSSION

Fracture toughness

It is customary to express K_{Ic} as a function of $\dot{a}$, in the following form:

$$K_{Ic}=A\dot{a}^n \quad (6)$$

where A and n are constants. This relationship can be theoretically explained by using a criterion of a constant crack opening displacement δ_c and considering the variation of E with $\dot{e}$[20]. However, dependence of K_{Ic} on $\dot{a}$ in thermosets presents a more complicated situation. The K_{Ic} *versus* $\dot{a}$ relationship cannot be derived by a constant crack opening displacement criterion since δ_c varies greatly with $\dot{e}$ and test temperature[2,5]. The K_{Ic} *versus* $\dot{a}$ (or $\dot{y}$) relationships illustrated in *Figures 1a–d* are the data of unmodified and rubber-modified epoxies showing type A and type B crack growth. With type A fracture, $\dot{a}$ is directly proportional to $\dot{y}$ (*Figure 2*). From *Figures 1c* and *1d* it was found that the slope dK_{Ic}/da of type A crack growth is close to zero or slightly negative. Mai and Atkins[21] have suggested that a negative value of $dK_{Ic}/d\dot{a}$ leads to crack jumping, whereas continuous crack propagation occurs when $dK_{Ic}/d\dot{a}$ is positive. This suggestion does not seem to be applicable to the fracture data of this study. In type A crack growth, the fracture toughness is almost independent of rubber content. In fact, at low $\dot{y}$ (10^{-7}–10^{-5} $m\,s^{-1}$) the value of K_{Ic} for all rubber-modified samples cured by cycle (1) is approximately 2.8 $MN\,m^{-3/2}$ and decreases to 2.3 $MN\,m^{-3/2}$ at higher $\dot{y}$ (10^{-4}–10^{-3} $m\,s^{-1}$). A similar tendency was also found in rubber-modified specimens cured by cycle (2). Using compact tension specimens, Peyser and Steg[22] have obtained similar fracture toughness values for different rubber content and displacement rate between 8.3×10^{-7} and 8.3×10^{-5} $m\,s^{-1}$, but in this limited range they did not recognize the dependence on the displacement rate (*Figures 1b–d*).

The most striking effect caused by rubber content on the fracture behaviour is on the transitional crack propagation velocity $\dot{a}_t$, or the transitional displacement rate $\dot{y}_t$, where the mode of failure changes from type A to type B as $\dot{a}$ (or $\dot{y}$) increases. As the rubber content is increased from 5 to 15 phr, $\dot{y}_t$ increases by nearly three orders of magnitude (*Figure 3*). It is of interest to calculate $\dot{y}_t$ for the unmodified epoxy using the equivalence between time and temperature. According to Kinloch *et al.*[1], type A/type B transition occurs at $\dot{y}_{t0}=8.3\times10^{-7}$ $m\,s^{-1}$ at $T_0=35$°C for unmodified samples. Also, $\dot{a}$ is

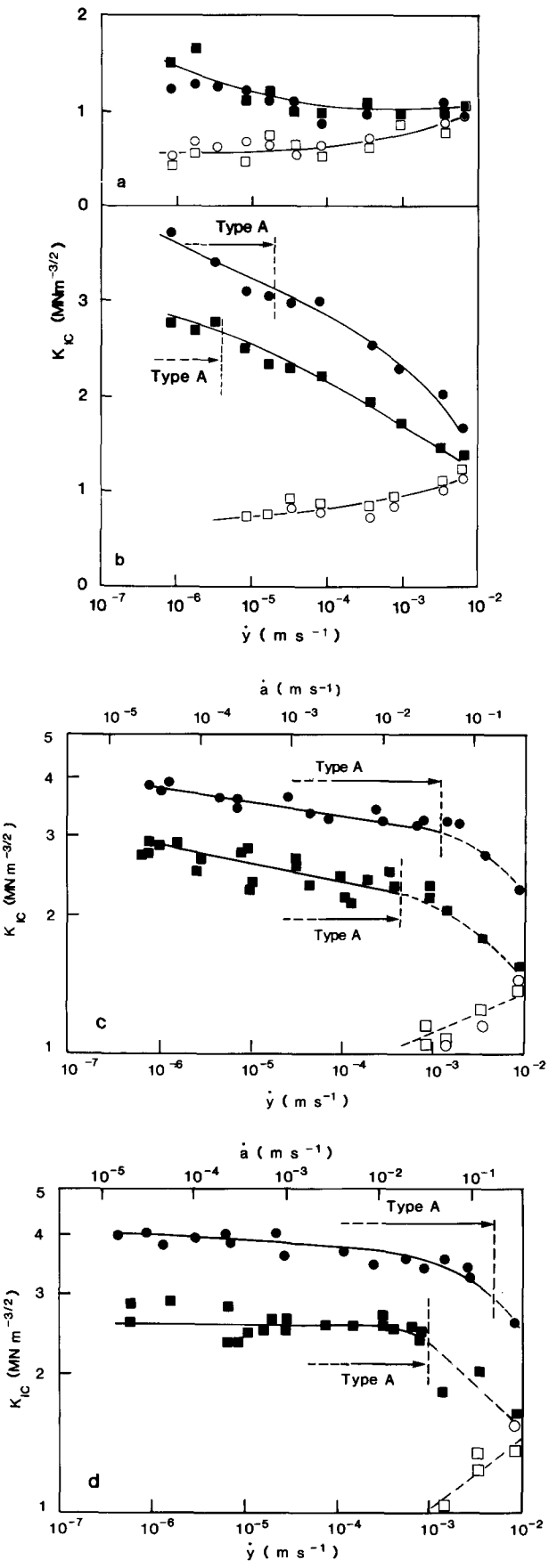

Figure 1 Relationship between stress intensity factor K_{Ic} and displacement rate $\dot{y}$ (and $\dot{a}$ where applicable) of the unmodified and rubber-modified epoxies. (a) Unmodified epoxy. (b–d) Rubber-modified epoxy: (b) 5 phr of rubber; (c) 10 phr of rubber; (d) 15 phr of rubber. Squares, specimens of cure cycle (1); circles, specimens of cure cycle (2). Full symbols, K_{Ic} (type A) or K_{Ici} (type B); open symbols, K_{Ica} (type B); superimposed symbols, K_{Ic} (type C)

related to the time to failure t_f by:

$$\dot{a} \propto 1/t_f \tag{7}$$

Therefore,

$$\frac{\dot{y}_{t0}}{\dot{y}_t} = \frac{\dot{a}_{t0}}{\dot{a}_t} = \frac{t_f}{t_{f0}} = a_T \tag{8}$$

where $\dot{a}_t$ and $\dot{a}_{t0}$ are the transitional crack velocities at

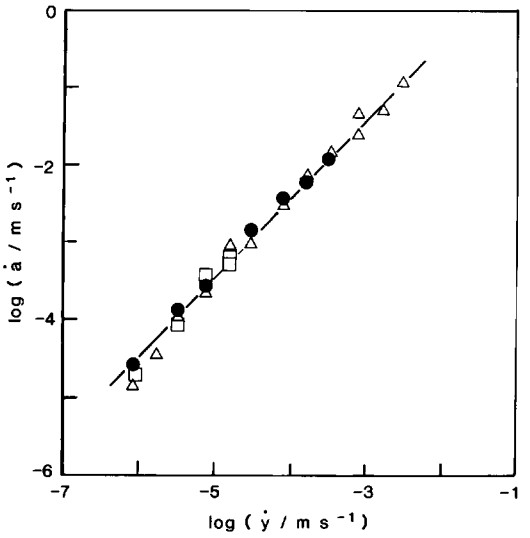

Figure 2 Relationship between crack propagation velocity $\dot{a}$ and displacement rate $\dot{y}$ of the rubber-modified epoxies at type A failure: (□) 5 phr of rubber; (●) 10 phr of rubber; (△) 15 phr of rubber

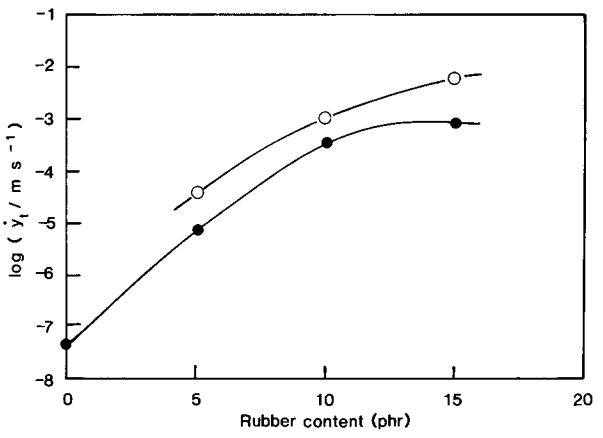

Figure 3 Effect of rubber content on the type A/type B transitional displacement $\dot{y}_t$; (●) specimens of cure cycle (1); (○) specimens of cure cycle (2)

room temperature and $T_0 = 35°C$, respectively. From the log a_T vs. T curve[6], a_T was found to be $10^{1.2}$. Substituting this figure in equation (8) gives $\dot{y}_t = 5.2 \times 10^{-8}$ m s^{-1}, which is well beyond the displacement rate of the testing machine. As shown in *Figure 3*, $\dot{y}_t$ increases rapidly with the rubber content up to 10 phr, then levels off. Accordingly, a rubber content ranging from 10 to 15 phr can be considered the optimum quantity where high values of K_{Ic} and $\dot{y}_t$ of the resultant rubber-modified samples are achieved while other mechanical properties are maintained at an acceptable level.

Comparing the modified and unmodified samples, the above results clearly indicate that, with a minimal decrease in Young's modulus, yield strength and glass transition temperature (*Table 2*), the addition of rubber to epoxy resin offers dual effects in improving the fracture behaviour, i.e. (1) enhancement of the fracture toughness, and (2) stabilization of crack propagation. The experimental results have demonstrated that increasing $\dot{y}$ or decreasing the temperature[1,2] or rubber content is equivalent to transition of the fracture modes from type A, type B and type C in that order.

Moreover, the curing history is another important factor influencing the fracture behaviour of rubber-modified epoxies. As shown in *Figure 1*, the K_{Ic} *versus* $\dot{a}$ relationships of specimens cured by cycle (2) clearly indicate further improvement in the two aspects of the fracture behaviour: (1) a higher K_{Ic}, and (2) a wider range of crack propagation velocity where the failure occurs in a ductile manner, i.e. higher $\dot{a}_t$, while other physical and mechanical properties such as Young's modulus, yield stress and glass transition temperature remain almost unchanged (*Table 2*). In comparison with specimens cured by cycle (1), the fracture data of specimens cured by cure cycle (2) indicate a 30–50% improvement in K_{Ic} and a 3–10 times increase in $\dot{a}_t$. In fact, the K_{Ic} value of specimens of 15 phr rubber is increased to 4 MN m$^{-3/2}$, which is extremely high for epoxies.

It is of interest to note that the molecular weight between crosslinks M_c calculated from the rubbery modulus E_r or the glass transition temperature T_g is almost independent of the curing history (*Tables 2* and *3*). This finding is different from the recent work by Kinloch *et al.*[12]. They suggested that the enhancement in K_{Ic} results from 7- to 8-fold increase in M_c of both unmodified and rubber-modified epoxies calculated from the 3-fold decrease in E_r. In considering the effect of cure history, two factors can be considered: the morphology of the second phase and the network structure of the epoxy matrix. In the present case, it appears that M_c is

Table 2 Mechanical and thermal characterization data

Cure cycle	Rubber content (phr)	E^a (MN m^{-2})	e_y	$\sigma_{cy}{}^a$ (MN m^{-2})	$T_g{}^b$ (°C)	$M_c{}^c$ (g mol^{-1}) from T_g (eqn (1))
(1)	0	2880	0.060	85	91–100	358
	5	2690	0.056	81	84–98	371
	10	2480	0.060	76	84–101	366
	15	2280	0.056	68	82–97	379
(2)	0	2940	0.060	84	89–98	363
	5	2730	0.058	82	84–98	371
	10	2550	0.060	76	81–94	384
	15	2320	0.058	68	80–95	388

[a] At $\dot{y} = 3.3 \times 10^{-5}$ m s^{-1}
[b] Transition range from extrapolated onset to end
[c] Mean value of T_g range used

Table 3 Equilibrium rubbery modulus E_r and molecular weight between crosslinks M_c

Rubber content (phr)	E_{r1}/E_{r2}[a]	M_{c2}/M_{c1}[a]
0	1.4	1.7
5	1.1	1.2
10	1.6	2.5
15	0.7	0.6

[a] 1 and 2 denote cure cycles (1) and (2)

independent of the cure history when 'full cure' is effected (*Tables 2* and *3*). This fact is supported by a similar fracture toughness of samples cured by cycles (1) or (2) (*Figure 1a*). The apparent conflict between this finding and recent work by Kinloch *et al.*[12], which reported a significant increase in M_c for these materials cured for 6 h/160°C, would appear to lie in the unexpected kinetics of the cure of this system. We have found the T_g of the material cured for 3 h/150°C to be relatively low (78°C at the end of the transition) and to be unexpectedly increased at temperatures lower than the cure temperature (90°C after 13 days/80°C; 97°C after 16 h/120°C). The traditional explanation for lower T_g when DGEBA/piperidine systems are cured at higher temperatures (see, for example, Cuadrado *et al.*[23]) of different network structures or piperidine evaporation are clearly insufficient. Furthermore, in contrast to the T_g data of this study (*Table 2*) where the T_g of the epoxy remains practically unchanged under two different cure cycles, Kinloch *et al.*[12] found a large T_g difference of 12°C between specimens cured for 16 h/120°C and 6 h/160°C. Thus, it seems that the lower T_g of materials cured for 6 h/160°C could be attributed to incomplete reaction, leading to networks of larger M_c and unreacted pendant epoxy groups. Similarly, after the first stage of cure cycle (2) (2.5 h/150°C) the networks contain active groups, which react at lower temperature during the second stage (16 h/120°C) and increase the crosslink density. This yields materials that effectively have the same physical properties and T_g as those from cure cycle (1), but exhibit improved toughness ($K_{Ic}=4$ MN m$^{-3/2}$) similar to the materials (cured for 6 h/160°C) of Kinloch *et al.*[12].

In the cure cycles of this study the size of rubber particles is determined in the first few hours before the gel point, while the rest of the cure and post-cure are to ensure the full cure conditions of the matrix. As illustrated in *Figure 1a*, the fracture toughness of the unmodified epoxy cured under a full cure condition (i.e. cure cycle (1) or (2)) shows similar fracture data in a wide range of displacement rates $\dot{y}$. However, when the rubber is added to the epoxy, even at a concentration as little as 5 phr, the effect of the cure conditions on the fracture behaviour becomes remarkable (*Figures 1b–d*). Post-failure examination of rubber-modified specimens reveals that, regardless of the rubber content, the cavitated particle size of the specimens cured by cure cycle (2) are always larger than those of the specimens of cure cycle (1) (*Figure 4*). The size distribution of the cavitated rubber particles is shown in *Figure 5*. Preliminary results[24] indicate that the rubber particles of the cure cycle (2) materials exhibit higher degree of cavitation, which is the difference in the total volume between the cavitated and uncavitated rubber particles. Higher degree of cavitation and larger cavitated particles imply a larger reduction in the stress triaxiality of the surrounding matrix, which is, in turn, more ready to deform plastically via shear yielding. Secondly, there is the possibility that different cure cycles could result in different phase composition and interface properties. The cure cycle (2) could generate better compatibility between the rubber and epoxy, which optimizes the interfacial bonding, resulting in higher energy dissipation during fracture due to high debonding stresses[9].

Crack opening displacement

The crack opening displacement δ_c, which is a useful parameter to describe the geometry of the crack tip and examine the crack-tip blunting, can be estimated by:

$$\delta_c=(K_{Ic}/\sigma_{ty})^2 e_y \tag{9}$$

Because K_{Ic} and σ_{ty} are functions of rate, the calculation of δ_c should be based on the correlation between the displacement rate $\dot{y}$, crack propagation velocity $\dot{a}$ and the strain rate at the crack tip $\dot{e}_{tip}$. Williams[25] has expressed the relationship between $\dot{e}_{tip}$ and $\dot{a}$ by:

$$\dot{e}_{tip}=\pi(E/K_{Ic})^2 e_y^3 \dot{a} \tag{10}$$

In this study, e_y is found to be 0.056–0.060 (*Table 2*). From equation (10), the ratio between $\dot{a}$ and $\dot{e}_{tip}$ is approximately 2–3 orders of magnitude. Based on the relationship between $\dot{a}$ and $\dot{y}$ (*Figure 2*), $\dot{y}$ is five orders of magnitude smaller than the strain rate at the crack tip $\dot{e}_{tip}$. This result is different from that of Kinloch *et al.*[2], in which two orders of magnitude difference between $\dot{y}$ and $\dot{e}_{tip}$ was estimated.

As illustrated in *Figure 6*, plots of the true compressive yield stress σ_{cy} against the logarithm of the strain rate $\dot{e}$ for the unmodified and rubber-modified epoxies show a linear relationship. Extrapolated values of the yield stress are used when the strain rate at the crack tip $\dot{e}_{tip}$ exceeds 1. The calculated results of the crack opening displacement δ_c are shown in *Figures 7* and *8* for specimens cured by cure cycles (1) and (2). Two interesting aspects are revealed from the figures. Firstly, the values of δ_c increase with decreasing rate. The data obtained by Kinloch *et al.*[2] indicate that the crack opening displacement increases with increasing temperature. This again confirms the equivalence between time and temperature.

Secondly, although a criterion of a constant crack opening displacement for fracture processes does not exist in epoxy polymers, in rubber-modified epoxies a constant crack opening displacement seems to govern the fracture modes when the crack propagation changes from type A to type B. From *Figures 7* and *8*, the constant values of δ_c at the transition of fracture modes from type A to type B or vice versa were found to be 80 and 140 μm for specimens of cure cycles (1) and (2), respectively. The following equation is employed to examine these constants[26]:

$$K_{Ic}=(e_y\delta_c)^{1/2}E(\dot{e}_{tip}) \tag{11}$$

Because the yield strain e_y is largely insensitive to both strain rate and rubber content, and the crack opening displacement at transition is constant, the stress intensity factor at transition K_t should be proportional to Young's modulus E. In other words, the ratio of the stress intensity at transition, K_{ta}/K_{tb}, of two materials (a and b) with different rubber contents is theoretically equal to the ratio of the corresponding moduli, E_a/E_b. From the results shown in *Table 4*, the values of K_{ta}/K_{tb} correlate well

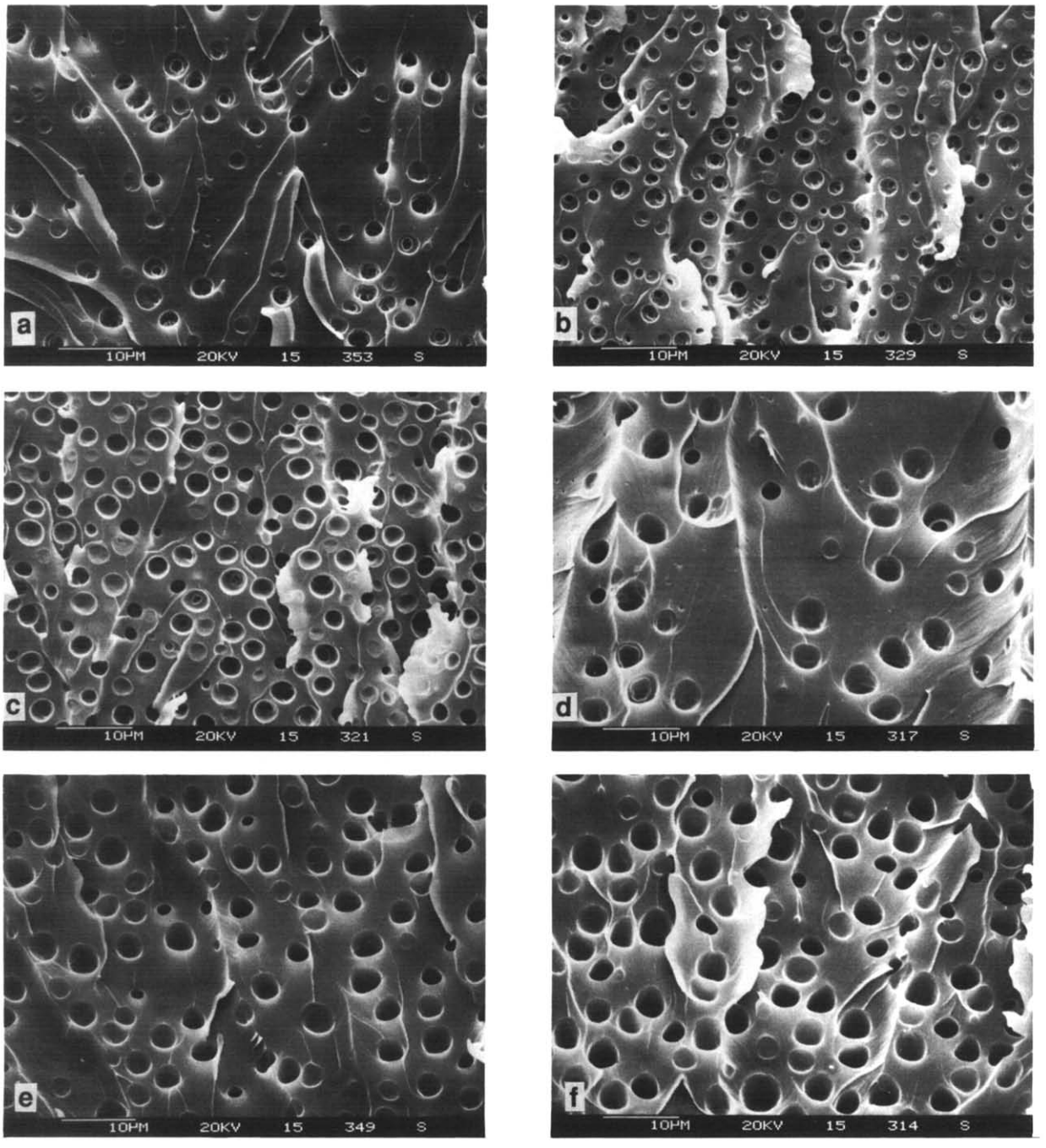

Figure 4 Fracture surface of the rubber-modified epoxies. Cure cycle (1): (a) 5 phr, (b) 10 phr, (c) 15 phr. Cure cycle (2): (d) 5 phr, (e) 10 phr, (f) 15 phr

Table 4 Comparison of K_{ta}/K_{tb} with E_a/E_b

Cure cycle	Rubber content (phr)	K_t (MN m$^{-3/2}$)	E^a (MN m^{-2})	K_{ta}/K_{tb}	E_a/E_b
(1)	5	2.5	2800	1.0[b]	0.98[b]
	10	2.5	2850	1.1[c]	1.02[c]
	15	2.2	2740		
(2)	5	3.0	2850	1.0[b]	0.99[b]
	10	3.1	2890	1.0[c]	1.04[c]
	15	3.0	2750		

[a] Modulus E is corrected for the $\dot{\epsilon}_{tip}$ at the transition
[b] 'a' denotes the specimen of 5 phr rubber and 'b' denotes the specimen of 10 phr rubber
[c] 'a' denotes the specimen of 5 phr rubber and 'b' denotes the specimen of 15 phr rubber

with the ratio of E_a/E_b. Further, since the yield strain e_y and the Young's modulus E are independent of curing history (*Table 2*), according to equation (11) the ratio of the stress intensity factors K_{t2}/K_{t1} of the specimens having the same rubber contents but cured differently is equal to the square root of the ratio of the crack opening displacement $(\delta_{t2}/\delta_{t1})^{1/2}$ at fracture transition (*Table 5*). Because the experimental error for K_{Ic} is within $\pm 5\%$, the error of the ratios K_{ta}/K_{tb} and K_{t2}/K_{t1} would be $\pm 10\%$ at most. Therefore, the equivalence between K_{ta}/K_{tb} and E_a/E_b, and between K_{t2}/K_{t1} and $(\delta_{t2}/\delta_{t1})^{1/2}$, amply justifies the existence of a constant crack opening displacement at fracture mode transition for the rubber-modified epoxies. It is noted that in the δ_c *versus* $\dot{y}$ curves (*Figures 7* and *8*) of the rubber-modified

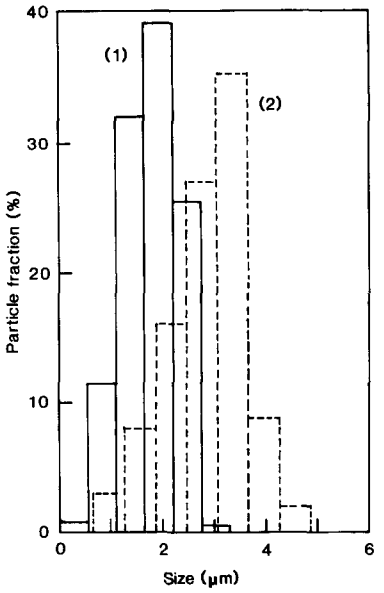

Figure 5 Typical size distribution of cavitated rubber particles (over 300 particles) for rubber-modified specimens (10 phr rubber): (1), cure cycle (1); (2), cure cycle (2)

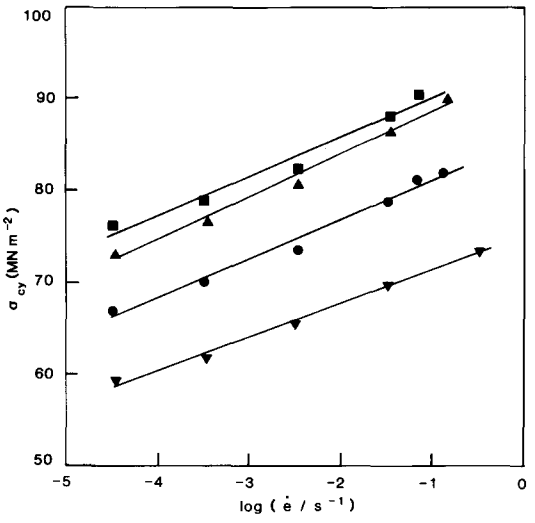

Figure 6 Compressive yield strength σ_{cy} *versus* logarithm of strain rate $\dot{e}$: (■) unmodified epoxy; (▲) 5 phr of rubber; (●) 10 phr of rubber; (▼) 15 phr of rubber

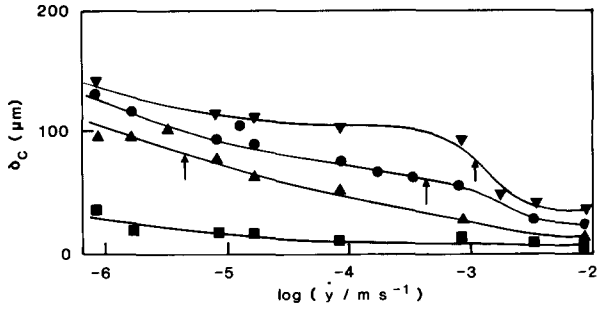

Figure 7 Relationship between the crack opening displacement δ_c and the displacement rate $\dot{y}$ for specimens of cure cycle (1). The arrow indicates the type A/type B transition of the failure mode. Symbols as in *Figure 6*

specimens (15 phr rubber) there exists a sudden decline in δ_c at the transition due to a substantial decrease from K_{Ic} of type A to K_{Ici} of type B.

Arrest line of type B crack growth (stick/slip)

The arrest line of stick/slip propagation of unmodified epoxies has been examined in detail by Yamani and Young[4], and Phillips *et al.*[27]. These authors have suggested that when stick/slip crack propagation occurs the crack propagates slowly through a region having the size of a Dugdale plastic zone Δ after the crack arrest line. The size of the slow-growth zone l_c, which is in good agreement[4] with the theoretical Δ, is a useful parameter to identify the actual size of the plastic zone. Nevertheless, the fracture pattern of the unmodified epoxies, as observed with a scanning electron microscope, presents various features, such as fine markings, secondary arrest lines and longitudinal lines, which cause considerable difficulties in determining the size of the slow-growth zone. On the other hand, the arrest line of the rubber-modified epoxies is characterized by stress whitening. The arrest region reveals massive cavitation of the rubber particles, indicating failure and deformation mechanisms of type A crack growth.

Stick/slip propagation undergoes the following steps of crack growth. After the crack arrest, the crack tip becomes blunt and the plastic zone, characterized by the cavitation of the rubber particles, is formed ahead of the blunt crack tip. As the load increases, a new crack is initiated and propagates through the plastic zone. The crack growth is type A and therefore the crack propagation velocity $\dot{a}$ through the plastic zone is directly proportional to the displacement rate $\dot{y}$. When the crack tip reaches the undeformed bulk material the crack tip rapidly jumps forward because the external energy is wholly converted into kinetic energy of crack propagation. From this argument, the failure modes seem to be controlled by a competition between $\dot{a}$ and the formation rate of the plastic zone. When $\dot{a}$ is lower than the formation rate, type A failure is predominant. Conversely, at high displacement rate the crack is initiated and

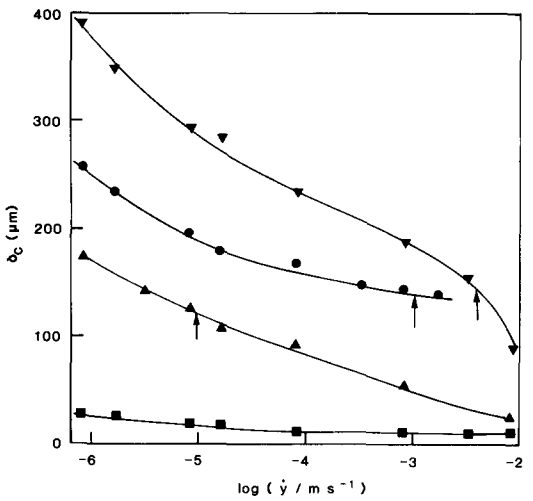

Figure 8 Relationship between the crack opening displacement δ_c and the displacement rate $\dot{y}$ for specimens of cure cycle (2). The arrow indicates type A/type B transition of the failure mode. Symbols as in *Figure 6*

Table 5 Comparison of the K_t ratio and the δ_t ratio

Rubber content (phr)	K_{t2}/K_{t1}[a]	$(\delta_{t2}/\delta_{t1})^{1/2}$[a]
5	3.0/2.5 = 1.2	1.35
10	3.1/2.5 = 1.2	1.35
15	3.0/2.2 = 1.4	1.35

[a] 1 and 2 denote cure cycles (1) and (2); $\delta_{t2} = 140$ μm and $\delta_{t1} = 80$ μm; K_t values are as in *Table 4*

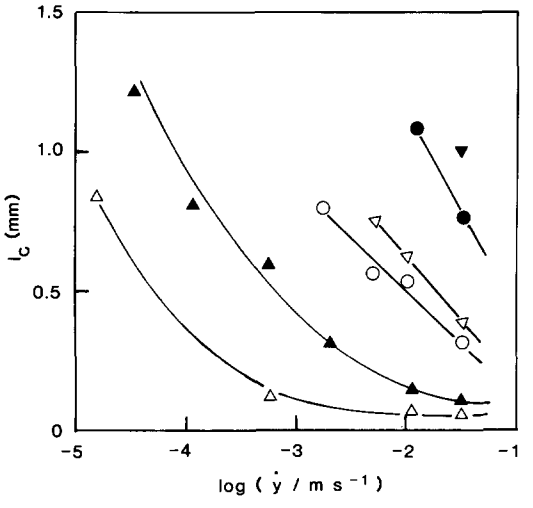

Figure 9 Relationship between the length of the slow growth zone in type B failure, l_c, and the displacement rate $\dot{y}$ of the rubber-modified epoxies: (△, ▲) 5 phr of rubber; (○, ●) 10 phr of rubber; (▽, ▼) 15 phr of rubber. Open symbols, cure cycle (1); full symbols, cure cycle (2)

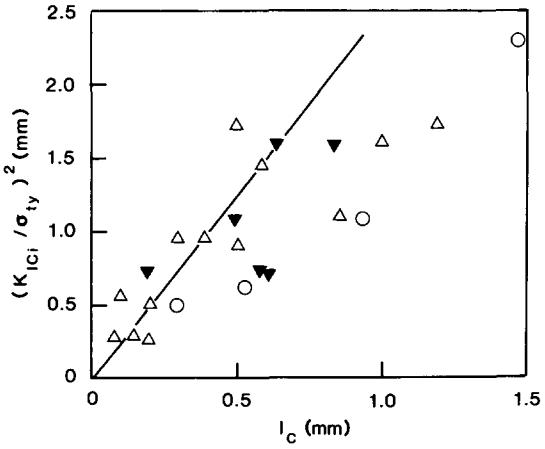

Figure 10 Plot of $(K_{Ici}/\sigma_{ty})^2$ *versus* the size of the slow-growth zone l_c for the rubber-modified epoxies: (△) 5 phr of rubber; (○) 10 phr of rubber; (▼) 15 phr of rubber. The straight line is equation (12)

Table 6 Comparison of l_t and Δ_t at the transition of the fracture mode

Rubber content (phr)	Cure cycle (1)		Cure cycle (2)	
	l_t (mm)	Δ_t (mm)	l_t (mm)	Δ_t (mm)
5	0.84	0.55	1.20	0.95
10	0.80	0.55	1.10	0.95
15	0.76	0.55	1.00	0.95

propagates so rapidly that there is insufficient time for the formation of the plastic zone. In this case type C failure occurs. A typical fractured surface of this type is featureless in unmodified epoxies or a smooth surface with uncavitated rubber particles in rubber-modified epoxies. As a result, type B failure can be considered as a mixed mode of type A and type C.

Figure 9 illustrates the relationship between the experimental value of l_c and $\dot{y}$. Since l_c is theoretically proportional to the crack opening displacement, the decreasing zone size, with the displacement rate $\dot{y}$, is consistent with the relationship between δ_c and $\dot{y}$ (*Figures 7* and *8*). Compared to specimens of cure cycle (1), specimens of cure cycle (2) have higher values of l_c, demonstrating a larger plastic deformation, which is consistent with a higher fracture toughness of the cure cycle (2) materials. Furthermore, a substantial increase in l_c is observed when the rubber content is increased. For example, for specimens of cure cycle (1) at $\dot{y}=3.33\times10^{-3}$ m s^{-1} the value of l_c increases from 80 to 760 μm as the rubber content increases from 5 to 15 phr. Since Δ can be expressed by[26]:

$$\Delta=\tfrac{1}{8}\pi(K_{Ic}/\sigma_{ty})^2 \qquad (12)$$

it is of interest to examine the correlation between Δ and l_c by plotting l_c against $(K_{Ici}/\sigma_{ty})^2$ for the rubber-modified epoxies of two cure cycles (*Figure 10*). In this figure, deviations from the straight line of exact equivalence increase as the fracture mode approaches the fracture transition from type B ($l_c>0.5$ mm), but the observed slow-growth zone (l_c) is in good agreement with Δ below $l_c=0.5$ mm. Since $(K_{Ic}/\sigma_{ty})^2$ is a function of $\dot{y}$, scatter of data in the high l_c region ($l_c>0.5$ mm) results from the strong dependence of l_c on rubber content and cure schedule as illustrated in *Figure 9*.

In the previous section, a constant crack opening displacement has been found at the type A/type B transition. Since the crack opening displacement δ_c is proportional to the plastic zone size (Δ) (equations (9) and (12)), a corresponding constant for Δ at the fracture mode transition should exist. Indeed, by using $\delta_{t1}=80$ μm for cure cycle (1) and $\delta_{t2}=140$ μm for cure cycle (2), the calculated values of the plastic zone size at the transition Δ_t are 0.55 and 0.95 mm, respectively. *Table 6* compares the calculated Δ_t and experimental l_t (l_c value at the type A/type B transition). The good agreement between the values further confirms the concept of constant crack opening displacement and plastic zone size at the transition of fracture mode.

CONCLUSIONS

Crack propagation in unmodified and rubber-modified epoxies has been shown to be a function of the displacement rate $\dot{y}$ (or the crack propagation velocity $\dot{a}$ for type A crack growth). Within $\dot{y}=8.3\times10^{-7}$ to 8.3×10^{-3} m s^{-1} and at room temperature the unmodified epoxies exhibit type B/type C crack growth, whereas the rubber-modified epoxies show type A/type B crack growth. Although the rubber content has little influence on the fracture toughness of the rubber-modified epoxies, the most striking effect of the rubber content on the fracture behaviour is on the transition of the fracture modes. The transitional displacement rate $\dot{y}_t$ (or the transitional crack propagation velocity $\dot{a}_t$), at which the fracture mode changes from type A to type B, increases with increasing rubber content. This implies that the rubber second phase not only enhances the fracture toughness but is also involved in the stabilization of the crack growth. On the other hand, the cure schedule has a profound effect on the fracture behaviour of the rubber-modified epoxies but not the unmodified materials. In particular, by using a high-temperature cure cycle (cycle (2)), not only did K_{Ic} reach 4 MN m$^{-3/2}$, but also the transitional rate parameter ($\dot{a}_t$ or $\dot{y}_t$) was enhanced compared to that of the sample of the same composition cured at lower temperature (cycle (1)). The fracture toughness of epoxy system can be influenced by two factors: (a) ductility of the matrix relating to M_c of the networks, and (b) the second-phase morphology. In this study, however, it has been found that M_c remains

unchanged under two different cure cycles, but larger uncavitated and cavitated rubber particles were observed in the cure cycle (2) materials. At present, the relation between cure history, second-phase morphology and fracture behaviour of the present epoxy system is unclear. Further study to investigate the enhancement of fracture toughness in terms of degree of cavitation in the rubber phase and the influence of cure history on the rubber/matrix interfacial bonding is necessary.

Data on the yield behaviour, Young's modulus and the interrelation among the crack propagation velocity, displacement rate and strain rate at the crack tip have been used to calculate the crack opening displacement δ_c as a function of the displacement rate $\dot{y}$. The size of the arrest line in type B crack growth is comparable to the theoretical Dugdale plastic zone, although deviation from the exact equivalence was observed as type B approaches type A. Furthermore, a constant crack opening displacement and plastic zone size was found at the type A/type B transition. Also, some evidence for the time–temperature equivalence in the fracture behaviour has been revealed from the fracture toughness and crack opening displacement data.

ACKNOWLEDGEMENTS

The author is indebted to Drs C. E. M. Morris and J. R. Brown for reading the manuscript and suggestions, and to Dr B. C. Ennis for helpful discussions.

REFERENCES

1 Kinloch, A. J., Shaw, S. J., Tod, D. A. and Hunston, D. L. *Polymer* 1983, **24**, 1341
2 Kinloch, A. J., Shaw, S. J. and Hunston, D. L. *Polymer* 1983, **24**, 1355
3 Kinloch, A. J. and Williams, J. G. *J. Mater. Sci.* 1980, **15**, 987
4 Yamani, S. and Young, R. J. *J. Mater. Sci.* 1980, **15**, 1823
5 Gledhill, R. A., Kinloch, A. J., Yamani, S. and Young, R. J. *Polymer* 1978, **19**, 574
6 Hunston, D. L., Kinloch, A. J., Shaw, S. J. and Wang, S. S. in 'Adhesives Joints' (Ed. K. L. Mittal), Plenum Press, New York, 1984, p. 789
7 Kinloch, A. J. and Hunston, D. L. *J. Mater. Sci. Lett.* 1987, **6**, 131
8 Manzione, L. T., Gillham, J. K. and McPherson, C. A. *J. Appl. Polym. Sci.* 1981, **26**, 889
9 Manzione, L. T., Gillham, J. K. and McPherson, C. A. *J. Appl. Polym. Sci.* 1981, **26**, 907
10 LeMay, J. D., Swetlin, B. J. and Kelley, F. N. ACS Symp. Ser. 243 (Eds S. S. Labana and R. A. Dickie), 1984, p. 165
11 Pearson, R. A. and Yee, A. F. *Polym. Mater. Sci. Eng.* 1983, **49**, 316
12 Kinloch, A. J., Finch, C. A. and Hashemi, S. *Polym. Commun.* 1987, **28**, 322
13 Nielsen, L. E. *J. Macromol. Sci. (C)* 1969, **3**, 69
14 Wright, W. W. *Br. Polym. J.* 1983, **15**, 224
15 Kinloch, A. J. and Young, R. J. 'Fracture Behaviour of Polymers', Applied Science, London, 1983, Ch. 3
16 Young, R. J. and Beaumont, P. W. R. *J. Mater. Sci.* 1977, **12**, 684
17 Outwater, J. O., Murphy, M. C. and Kumble, R. G. ASTM STP 559, 1974, p. 127
18 Murphy, M. C., Kumble, R. G., Berry, J. T. and Outwater, J. O. *Am. Foundrymens Trans.* 1973, **81**, 158
19 Wronski, A. S. and Pick, M. *J. Mater. Sci.* 1977, **12**, 28
20 Young, R. J. and Beaumont, P. W. R. *Polymer* 1976, **17**, 717
21 Mai, Y.-W. and Atkins, A. G. *J. Mater. Sci.* 1975, **10**, 2000
22 Peyser, P. and Steg, Y. *J. Adhesion* 1988, **25**, 133
23 Cuadrado, T. R., Almaraz, A. and Williams, R. J. J. 'Crosslinked Epoxies' (Eds B. Sedlacek and J. Kahovec), de Gruyter, Berlin, 1987, p. 179
24 Truong, V.-T., unpublished data
25 Williams, J. G. *Int. J. Fract. Mech.* 1972, **8**, 393
26 Williams, J. G. *Adv. Polym. Sci.* 1978, **27**, 67
27 Phillips, D. C., Scott, J. M. and Jones, M. *J. Mater. Sci.* 1978, **13**, 311